ANALYSIS OF TIME-SERIES BACKSCATTER OF ERS-2 C-BAND SCATTEROMETER OVER THE *THAR* DESERT IN INDIA

C. P. Singh [a], D. G. Trivedi [b], Shiv Mohan [a] *, Ajai [a]

[a] Environment, Forestry and Microwave Applications Division (EFMD), Forestry, Land use Planning and Photogrammetry Applications Group (FLPG), Remote Sensing Applications and Image Processing Area (RESIPA), Space Applications Centre, ISRO, Ahmedabad-380015 – (cpsingh, shivmohan, ajai)@sac.isro.gov.in
[b] Physics Department, St Xaviers College, Gujarat University, Ahmedabad-380009 - dgtrivedi60@rediffmail.com

KEY WORDS: Scatterometer, ERS-2, *Thar*, Dunes, Backscattering coefficient, time series.

ABSTRACT:

Space-borne wind scatterometers are important element of microwave remote sensing systems because of their proven ability to make all-weather measurements of wind vector over the ocean. In addition to this, scatterometer have also been investigated for land applications. A portion of hot ("*Thar*") desert in India is studied for its time-series backscatter response. Major dunes types were identified and their temporal trends were studied. The year 2000 scatterometer data of ERS-2 C-band over this region showed the variability of backscattering coefficient of the order of 11.27 dB (-20.08 to -8.71 dB). These variations were analyzed in terms of scattering due to various factors like soil moisture, vegetation, rainfall, and surface roughness. For this purpose, nine dune signatures over six types of sand dunes have been studied. In general, high backscattering was observed in the months of July – August and low backscattering was observed in the months of May – June. The study indicated the potential of C-band scatterometer data for monitoring temporal variability for modelling and monitoring desert ecosystem. Further, potential of the C-band data for monitoring the aerodynamic roughness length (Z_0) over Indian *Thar* desert was also established.

1. INTRODUCTION

Optical as well as microwave remote sensing data have been successfully used for monitoring and mapping of deserts all over the world. In optical bands, the desert shows higher reflectance whereas in microwave frequencies active sensor shows low backscattering coefficient values and passive sensors show high brightness temperature values (Mishra *et al*, 2002). Among the space-borne SAR systems, C-band data is widely used for various land applications due to availability of ERS-1/2, Radarsat, and Envisat SAR. In addition to this, scatterometer from ERS-1/2 operating at C-band and QuikScat operating at Ku band have also been investigated for land applications (Birrer *et al*, 1982; Drinkwater *et al*, 2000 & 2001; Kennett *et al*, 1989; Kerr *et al*, 1993; Long *et al*, 1994, 1999; Mougin *et al*, 1995; Prigent *et al*, 2005; Wagner *et al*, 1999a, 1999b; Wismann, 1998). Spaceborne scatterometers have provided continuous synoptic microwave coverage of earth for nearly one and half decade.

A scatterometer measures the normalized radar cross-section (NRCS) or backscattering coefficient of earth's surface, also termed sigma-nought (σ^o), a dimensionless quantity. For ocean, the backscatter is due to Bragg scattering of microwaves from centimetre length capillary ocean waves which is related to the wind. For land surface, the backscatter is due to the surface roughness and dielectric properties as well as volume scattering from vegetation. The scatterometer onboard ERS-1/2 operates at C-band in VV-polarization mode with 25 to 50 km spatial resolution over 500 km swath. This coarse resolution (~50 km) of the scatterometer measurements is a major drawback in studies over land surfaces. However, enhanced resolution product from Brigham Young University (BYU) is able to provide 8.9 km spatial resolution datasets, which have been generated using the scatterometer image reconstruction (SIR) resolution enhancement algorithm (Early *et al*, 2001; Long *et al*, 1993, Long and Hicks, 2005).

The present study has made use of this data for the year 2000 to analyse temporal changes in σ^o over Indian desert. Further, backscattering data is used to derive aerodynamic roughness length (Z_0) over Indian *Thar* Desert area. The scatterometer data available in "sir" format was converted to Geotiff using IDL (the Interactive Data Language) script and Indian region data was extracted. The data was available in the form of radar σ^o. ERS-2 σ^o image (values in dB at 40° incidence angle) of Indian region were co-registered with SPOT-4 (VEGETATION) NDVI data. In addition, digital elevation model, temperature and rainfall data was also used for interpretation of the σ^o variation. The aerodynamic roughness length, Z_0 was also modelled using a log-linear model (Prigent *et al* 2005), which uses σ^o.

1.1 The Instruments

A scatterometer is incoherent radar that measures reflectivity over a set of different incident angles. The Active Microwave Instrument (AMI) flown on ERS-2 operates at C-band (5.3 GHz) and uses three antennas with vertical polarization (VV) in the scatterometer mode. They are looking 45° forwards (Fore beam), sideways (Mid beam), and 45° backwards (Aft beam) with respect to the satellite flight direction. The incidence angle of the radar ranges from 18° to 57°, illuminating a 500 km wide swath on the right hand side of the satellite track. The along-track and cross-track spatial resolution is 50 km (Wismann, 1998). Enhanced resolution images from ERS-2 data use the Scatterometer Image Reconstruction (SIR) algorithm. In the processing, a linear model relating σ^o and incidence angle is assumed, i.e. $\boldsymbol{s}^\circ(dB) = A + B(\boldsymbol{q} - 40)$ where A is the "incidence angle normalized σ^o" at 40° incidence in dB, B is the effective incidence slope of σ^o versus incidence angle in dB/deg, and $\boldsymbol{q}$ is the incidence angle of the observation. The SIR algorithm makes images of A and B on an 8.9 km pixel grid. The effective resolution is estimated to be 20-30 km

---

* Corresponding author

resolution, depending on region and sampling conditions. Raw ERS measurements have a quoted nominal resolution of 50 km on a 25 km sampling grid.

Because the AMI SAR and scatterometer modes are mutually exclusive, the resulting coverage gaps produce reduced quality images when the SAR mode is operated over the study area. In producing ERS-2 SIR images, multiple passes of the spacecraft are combined to produce a higher spatial resolution (at a cost of reduced temporal resolution). The overlapped processing enables true resolution enhancement of the images. In combining the multiple passes, σ^o is assumed to be independent of azimuth angle.

2. STUDY AREA

The study area is Indian part of the *Thar* desert, which is located between $24^o 36'$ – $29^o 21'$ N Latitude and $69^o 32'$ - $75^o 26'$ E Longitude (fig.1). The *Thar* Desert (also known as the "Great Indian Desert") in India, is geographically, located in the state of Rajasthan, between the foothills of the Aravalli -
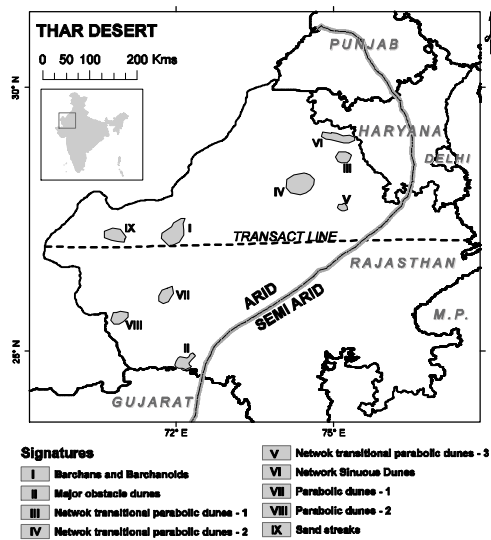
Figure 1. Study Area and Signatures (the *Thar* Desert)

ranges in the east and the international border with Pakistan in the west. It lies mostly in the Indian state of Rajasthan, and extends into the southern portion of Haryana and Punjab states and into northern Gujarat state. The *Thar* desert is bounded on the northwest by the Sutlej River, on the east by the Aravalli Range, on the south by the salt marsh known as the Rann of Kutch (parts of which are sometimes included in the *Thar*), and on the west by the Indus River. Depending on the areas included or excluded, the nominal size of the *Thar* can vary significantly. According to the WWF definition, the *Thar* has area of 238,700 km². Another source gives the area of 446,000 km² extending 805 km long and about 485 km wide, with 208,110 km² in India. Of the Indian portion, 61% falls in Rajasthan, 20% in Gujarat and 9% in Punjab and Haryana combined.

The *Thar* desert is dominated by the south-west monsoon, which controls both the wind vector and the vegetation cover. The configuration of atmospheric dynamics and sinking air masses in the region inhibit rain in this region despite the fact that considerable precipitable moisture exists in the atmosphere. Minor changes in the atmospheric circulation patterns result in amplified changes in the rainfall, the winds and the aeolian

dynamism. It is an austere area where water is scarce and occurs at great depths, from 30 to 120 m below the ground level. The region is dominated by aeolian bedforms of different dimensions, including the sand dunes. The thickness of aeolian cover can range from 1m to 100 m. Westward the natural vegetation becomes gradually sparse, cultivation on dune slopes becomes less frequent, and reactivation of the high dunes are more recurrent. Aeolian activity in the *Thar* desert is mainly restricted to the period of summer winds associated with the south west monsoon. The north eastern wind of winter months plays only a minor role in aeolian activity and is largely limited to the northern fringe of the desert. Strong sand and dust shifting winds begin from March onwards when the surface is dry and maximum wind speed (20 km/h or more) is reached at all the meteorological stations during June. May and July are also very windy. Since this is also the period when much of the ground flora is dry, the environment is suitable for aeolian activities. The wind and the sand dynamics cease with the arrival of monsoon rains (end of June along the eastern margin of the desert, and mid-July in the western part). Although higher wind strength and lower rainfall favour erosivity of the wind (Singhvi and Kar 2004).

Sand dunes of the *Thar*: Sand dunes are the most spectacular aeolian bedforms in the *Thar* desert. As in other deserts, the genesis of different types of dunes is the result of a delicately balanced relationship between the strength, direction and the duration of wind, sediment supply, rainfall, vegetation cover and land surface conditions. Commonly, dunes are classified according to their form as transverse dunes, barchan dunes, barchanoid dunes, parabolic dunes, longitudinal dunes and star dunes. Transverse dunes are long with straight crests and they migrate along the prevailing wind direction and tend to form when there is an abundant sand supply. Barchan dunes are curved like horseshoes and migrate with their arms pointing in the downwind direction. Barchan dunes form when there is limited sand available and the area between dunes is generally flat and void of sand. Sometimes they become laterally attached and form barchanoid dunes. Longitudinal dunes are dunes that elongate in the direction parallel to the prevailing winds. These dunes lack steep lee slopes and are almost symmetrical in the direction across their length. Longitudinal dunes tend to develop where the prevailing winds vary seasonally but blow from adjacent quadrants. Compound dunes can form when two or more dunes of the same type are combined by overlapping or being superimposed. Complex dunes are those in which two different dune types coalesce or overlap. Three major dune types in *Thar* are the parabolic, transverse and linear dunes. A variety of network dunes, major obstacle dunes (along the hill slopes), barchans, barchanoids and megabarchanoids, and the sand streaks and zibars are also found (fig 2). Dominantly old dunes (fig.2) are mostly the products of past changes in climate. These dunes are usually 10 to 40 m high, and are now naturally stabilized. Since the average silt and clay content in the dunes is 10-15% of the total sediment weight, moisture-holding capacity of the dunes is high. The dunes, therefore, can sustain a good amount of natural vegetation. In contrast, the new dunes consist mostly of the crescentric barchans (2-8 m), the barchanoids (2-15 m) and the megabarchanoids (20-40 m), as well as some small dunes like the sand streaks etc., which are forming under the present arid condition in the western part of the desert (Singhvi and Kar 2004).

The soils of the Arid Zone are generally sandy to sandy-loam in texture. The desert soils occupy the districts of Jodhpur, Bikaner, Churu, Ganganagar, Barmer, Jaisalmer, and Jalore. The area is covered not only by sheet of sand but also of rocky

projections of low elevations which constitute the older rocks of the country.
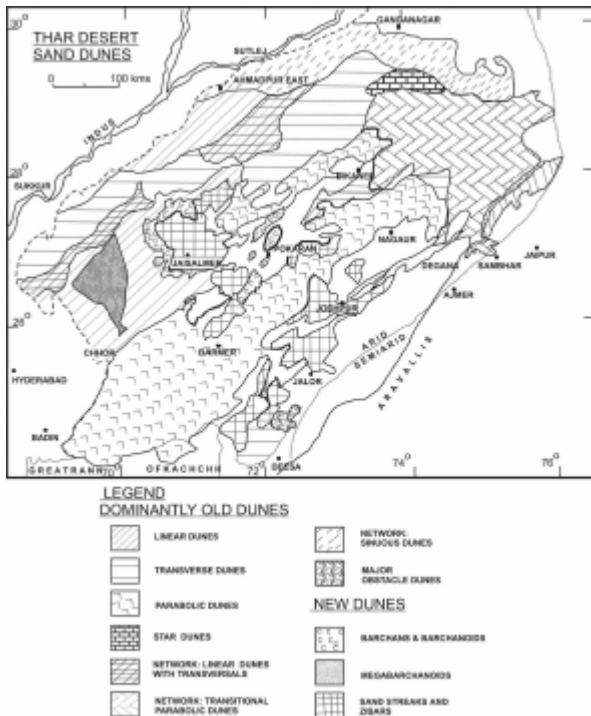
Figure 2. Dune types in the *Thar* (after Kar 1996).

3. MATERIALS AND METHODS

The South Asia chip data available from ERS-2 Scatterometer for year 2000 was used to generate the backscattering images of India. The scatterometer data was available in BYU-SIR format, which provide enhanced resolution to the extent of 8.9 km for ERS-2 C-band data. In addition to this, SPOT VEGETATION - NDVI product of same year was used in this study. All the scatterometer data and NDVI data were first co-registered. A portion of the *Thar* desert in India was extracted for its time-series backscatter response in relation to meteorological and biophysical parameters. For, identifying the major dune types in this desert region, corresponding dune map (Singhvi and Kar 2004) was used. For identifying the presence of vegetation, the Landsat data (ETM+) was visually interpreted. The SRTM DEM (90 m resolution) was also used to measure the height variation in the area. Subsequently, nine signatures over six types of sand dunes with or without vegetation were identified and signatures statistics were extracted and analysed. A transact profile was also generated from Shahgarh in Western portion to Aravallis (Near Jaipur) in the Eastern portion. Further, attempt was made to calculate the Z_0 using a log-linear model (Prigent *et al* 2005). The model estimates the Z_0 based on σ^o.

4. RESULTS AND DISCUSSION

The *Thar* desert presents picture of contrast in backscatter image in comparison to other land covers in India (fig.3). However variation in desertic terrain is assigned due to changes in dunes roughness (Singh, *et al* 2006). The data in year 2000 over this region showed the variability of σ^o of the order of 11.27 dB (-20.08 to -8.71 dB). These variations can be explained in terms of scattering due to various factors like soil moisture, vegetation, rainfall, and surface roughness due to wind. In general, high backscattering was observed in the

months of July – August and low backscattering was observed in the months of May – June (table.1 and fig.4).
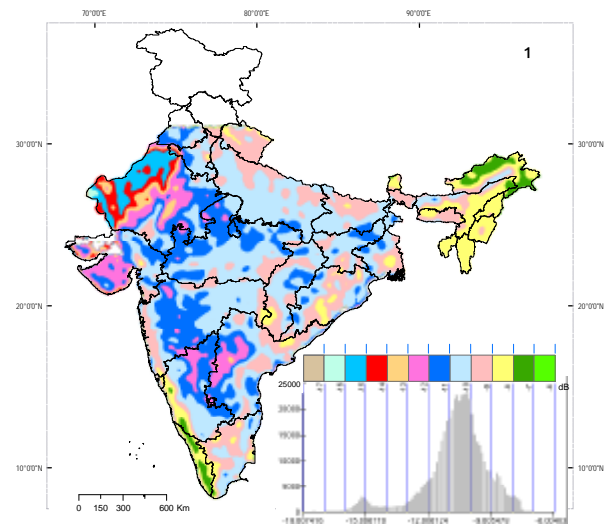
Figure 3. A sliced image map of January 2000 of ERS-2, C – band σ^o at 40° of incidence angle (reproduced from Singh *et al*, 2005)

Table 1: σ^o Variability in the *Thar* Desert (Year 2000)

S.N.	MONTHS	MIN σ^o (dB)	MAX σ^o (dB)	RANGE (dB)
1	January	-16.72	-9.97	6.745
2	February	-17.61	-10.07	7.531
3	March	-18.98	-9.92	9.06
4	April	-19.65	-9.98	9.67
5	May	-20.08	-9.98	10.1
6	June	-19.94	-9.86	10.08
7	July	-18.17	-8.76	9.406
8	August	-16.94	-8.71	8.233
9	September	-17.76	-9.70	8.059
10	October	-17.64	-10.35	7.295
11	November	-18.03	-9.94	8.095
12	December	-17.53	-9.91	7.611
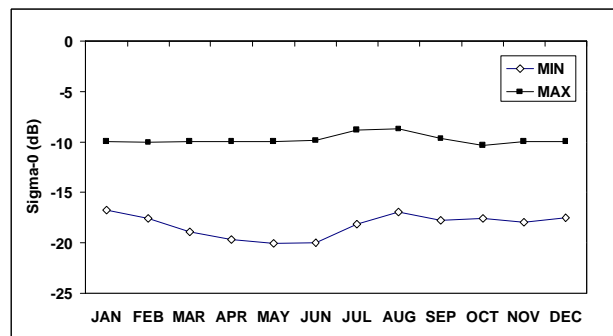
Figure 4. Variability of σ^o over the year 2000.

Spatial and temporal variation: In sand-dune areas, the minimum σ^o is observed in the last week of June, which is attributed due to dry soil moisture conditions. During this period the NDVI value is also found at the lowest order. The maximum σ^o observed, attributed mostly due to presence of vegetation in the second week of September.

In areas of sand dunes with-vegetation the minimum σ^o observed is in the last week of May, that is -19.5 dB, which is attributed due to no soil moisture (rainfall – nil) and high mean temperature (around 36.8^o C). During this period the NDVI value is also found at the lowest order (0.16). The maximum σ^o observed in this area is -12.7 dB mostly due to comparatively less temperature (31.6^{o}C) followed by increased NDVI (0.27).

The σ^o shows a gradual decrease until last week of June, afterwards a sudden increase in σ^o is found up to July – August, as the moisture level increases due to arrival of monsoon in this region (fig. 5). Onset of monsoon suddenly increases the soil moisture content, which leads to less transmission of energy through the medium and increase in surface scattering. From September onward σ^o decreases due to decrease in soil moisture attributed to percolation of water and high evaporation rate.
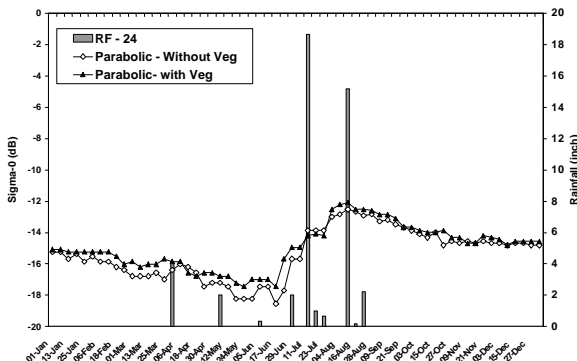
Figure 5. σ^o Vs Mean-24 hrs Rainfall (Parabolic Dunes)

The monthly averaged σ^o images over Thar desert and surrounding arid region are shown in Figure 6. The *Thar* desert-
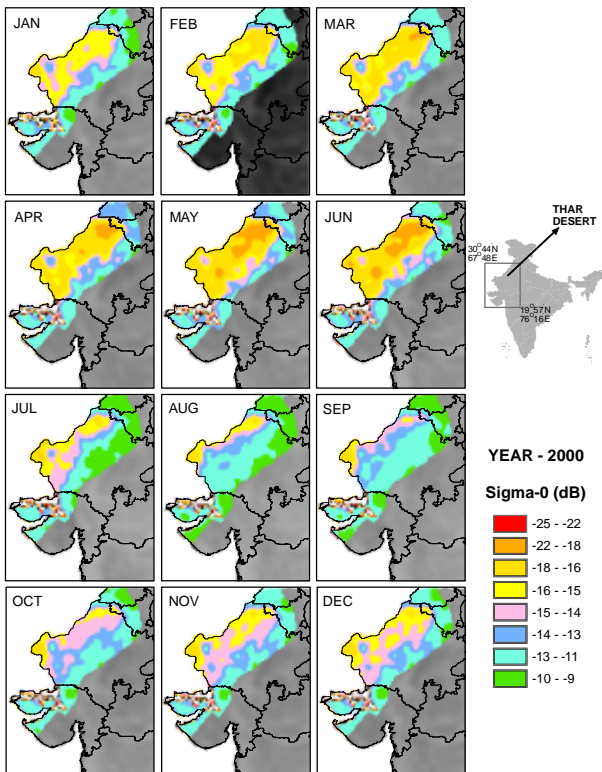
Figure 6. Monthly averaged σ^o over arid area including the *Thar* desert in the year 2000.

is characterized by low σ^o value (-25 to -13 dB), surrounded by (arid region) comparatively high σ^o value (-13 to -9 dB). The high σ^o value (-10 to -9 dB) has also been found over mountainous region, which is due to high topography (fig. 7). The low σ^o value is surrounded by high σ^o value, which shows sparse vegetation cover surrounded by the desert. During summer season the areal extent of low σ^o value is found to be more than other months of the year 2000.
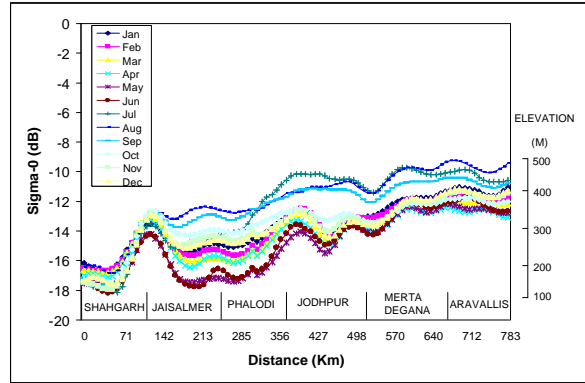
Figure 7. Transact Profile of σ^o values

The increase in σ^o values continue subsequently by the growth in vegetation and corresponding increase in surface roughness. Good correlation has been observed with σ^o and NDVI (fig 8). In summer months from the beginning of March, moisture content in desert region decreases significantly resulting in lower σ^o (fig.9).
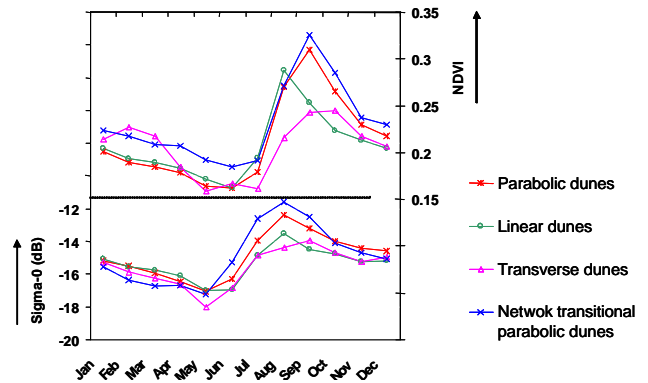
Figure 8. σ^o and NDVI response for dunes with vegetation.
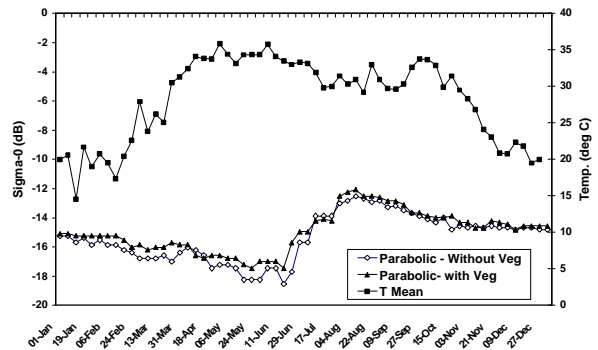
Figure 9. σ^o Vs Mean Temperature (Parabolic Dunes)

From figure 10 it is evident that the overall range of σ^o follows a cyclic pattern in almost all signatures under study. Due to physical scattering mechanism (surface roughness and

dielectric properties as well as volume scattering from vegetation) with dunes surfaces (attributing to variability in σ^o), it is possible to discriminate dune types. The discrimination of different sand dunes is best possible in the month of June (fig 11).
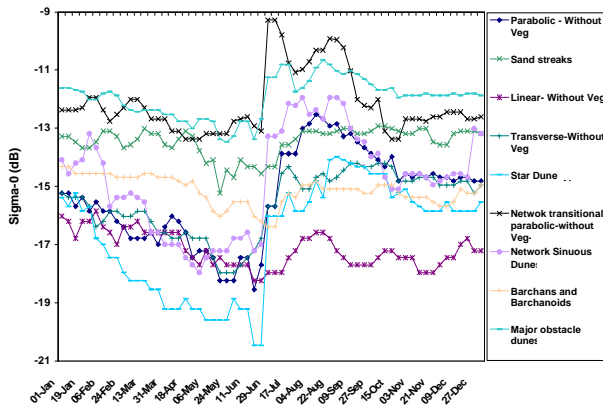
Figure 10. The *Thar* Desert's Different Dune Types: Backscatter Response
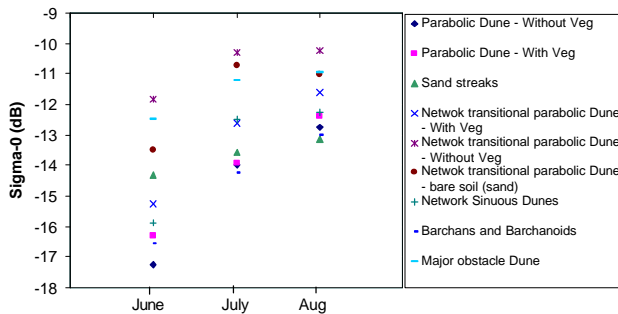
Figure 11. Separability of different dune types in the months of June July and August

Backscatter response to dunes types: A cyclic pattern in the *Thar* (fig.6) in general and all dune types studied (fig.10), in particular, have been observed. This pattern is mostly governed by the presence of moisture during rainy season and subsequently due to volume scattering by vegetation cover and then increase in temperature. Higher σ^o (-14 to -13 dB) range (blue colour in fig 6) may also be due to presence of some paleochannel loaded with moisture which needs to be validated.

The order of σ^o of different dune types studied (in increasing order) is as under:
Network transitional parabolic > Major obstacle > Network Sinuous > Parabolic > Barchans and Barchanoids > Sand streaks > Linear > Transverse > Star > Megabarchanoids

Aerodynamic roughness length, Z_0: The Z_0 is the height above a surface at which wind profile is zero and it was estimated using a model described by Prigent *et al* 2005. The Z_0 values obtained were varying from 0.01 cm to 0.34 cm with minimum value during May-June period. These variations are within the limits as described by Prigent *et al* 2005. Z_0 is the important parameter to study atmospheric circulation and aeolian sediment transport (in simple way it is wind patterns, wind erosion pattern and sand/soil shift patterns) (Greeley and Iversen, 1987).

5. CONCLUSION

C- band radar time-series backscatter response for year 2000 covering the *Thar* desert region was studied. The data showed the variability of σ^o of the order of 11.27 dB (-20.08 to -8.71 dB). Major dunes types were identified and their temporal trends were also studied. In general, high backscattering was observed in the months of July – August and low backscattering was observed in the months of May – June.

Over *Thar* desert region σ^o values is very low and vary gradually from summer season to rainy and winter seasons. The sharp change in moisture level in desert region is also reflected clearly from σ^o. It can also be concluded that the dune type separation using σ^o is best possible in the month of June. Time series analysis using scatterometer data over many years (decades) may give better insight of the formation of the dunes, "dune shift" and spread of desertification.

Further, potential of the C-band data for monitoring the aerodynamic roughness length, Z_0 over Indian *Thar* desert was found meaningful. The Z_0 estimated from σ^o can be used in climate and dust emission models. The dune spacing using SRTM-DEM and its relation with σ^o in the *Thar* can also be attempted in future. The study indicated the potential of C-band scatterometer data for monitoring temporal variability for modelling and monitoring desert ecosystem.

REFERENCES

Birrer, I.J., Bracalente, E.M., Dome, G.J., Sweet, J., and Berhold, G., 1982. σ^o signature of the Amazon Rainforest obtained from the Seasat Scatterometer, *IEEE Trans. Geosci., Remote Sensing,* 20(1), pp. 11-17.

Drinkwater, M.R., and Lin, C., 2000. Introduction to special section on emerging scatterometer applications, *IEEE Trans. Geosci., Remote Sensing,* 38(4), pp. 1763-1764.

Drinkwater, M.R., Long, D.G. and Bingham, A.W., 2001. Greenland Snow accumulation estimates from satellite radar scatterometer data, *Journal of Geophysical Research*, 106 (D24), pp. 33935-33950.

Early, David S. and Long, D. G., 2001. Image reconstruction and enhancement resolution imaging from irregular samples, *IEEE Trans. Geosci., Remote Sensing,* 39(2), pp.291-302.

Greeley, R. and Iversen, J., 1987. Measurement of wind fraction speed over lacva surfaces and assessment of sediment transport, Geophysical Research letter, 14, pp. 925-928.

Kar, A., 1996. Morphology and evolution of sand dunes in the Thar desert as key to sand control measures; *Indian Journal of Geomorphology,* 1(2), pp.177-206

Kennett, R.G., and Li, F.K., 1989. Seasat over – Land Scatterometer Data, Part I: Global overview of Ku-Band Backscatter Coefficients, *IEEE Trans. Geosci., Remote Sensing,* 27(5), pp. 592-605.

Kerr, Y. H. and Magagi, R. D., 1993. Use of ERS-1 wind scatterometer data over land surfaces: Arid and semi-arid lands(F1), Proc. Second ERS-1 Symposium – Space at the Service of our Environment, Hamburg, Germany, 11-14 Oct, (1993): pp. 383-388.

Long, D.G. and Drinkwater M.R., 1999. Cryosphere applications of NSCAT data, *IEEE Trans. Geosci., Remote Sensing,* 37(3), pp. 1671-1684.

Long, D.G., and Hardin, P., 1994. Vegetation studies of the amazon basin using enhanced resolution Seasat Scatterometer data, *IEEE Trans. Geosci., Remote Sensing,* 32 (2), pp. 449-460.

Long, D. G. and Hicks, B. R., 2005. Standard BYU QuikScat/SeaWinds Land/Ice Image Products, Revision 3.0, MERS Technical Report # MERS 05-04, ECEN Department Report # TR-L130-05.04.

Long, D. G., Hardin, P., and Whiting, P., 1993. Resolution enhancement of scatterometer data, *IEEE Trans. Geosci., Remote Sensing,* 31(3), pp.700-715.

Mishra, N.C., Kanwar, R., Sarkar, S., Dash, P., and Singh, R.P., 2002. Use of multi-sensor data for mapping of Thar desert, *Adv. Space Res.,* 29(1), pp. 51-55.

Mougin, E., Lopes, A., Frison, P. and Proisy, C., 1995. Preliminary analysis of ERS-1 wind scatterometer data over land surfaces, *Int. Jr. of Remote Sensing,* 16(2), pp. 391-398.

Prigent, C., I. Tegen, F. Aires, B. Marticorena, and Zribi M., 2005. Estimation of the aerodynamic roughness length in arid and semi-arid regions over the globe with the ERS scatterometer, *J. Geophys. Res.,* 110, D09205, doi:10.1029/2004JD005370.

Singh, C.P., Trivedi, D.G., Shiv Mohan, and Ajai, 2005. Land Cover Signature at C-Band Derived from ERS-2 Scatterometer, Proc. of 25th ISRS-2005 Annual Convention & National Symposium, 6-9 December 05, Ranchi, India. *(in press).*

Singh, C.P., Trivedi, D.G., Shiv Mohan, and Ajai, 2006. Comparison of Ku- and C-band radar backscatter signatures over Indian region, Proc. of Geomatics-2006 (National Conference on Geomatics for Infrastructure Development), 4-6 January 06, Chennai, India. *(in press).*

Singhvi, A.K. and Kar, A., 2004. The Aeolian sedimentation record of the *Thar* desert, Proc. Indian Acad. Sci. (Earth Planet Sci.), 113, No.3, September-2004, pp. 371-401.

Wagner, W., Lemoine, G. Borge, M. and Rott, H., 1999b. A study of vegetation cover effects on ERS scatterometer data, *IEEE Trans. Geosci., Remote Sensing,* 37(2), pp. 938-948.

Wagner, W., Noll, J., Bogeaud, M. and Rott, H., 1999a. Monitoring soil moisture over Canadian Praries with ERS Scatterometer, *IEEE Trans. Geosci., Remote Sensing,* 37(1), pp. 206-216.

Wismann, V., 1998. Land surface monitoring with space borne scatterometer. Proc. Joint ESA-Eumetsat Workshop on Emerging Scatterometer Applications – From research to operations. ESA SP-424: pp. 25-31.